Locating Earth-Faults in Compensated Distribution Networks by means of Fault Indicators

E. Bjerkan, T. Venseth

Abstract—This paper presents theory on transients generated during the initiation of earth-faults. The transients are used for detection and location of faults by means of fault-indicators. Electric and magnetic field measured by the indicator is shown to be a scalar/vectorial sum as a function of line configuration and heights above ground.

A field-test in a 22kV rural network is performed in order to investigate coherence with theory, by measuring phase voltages and currents together with the fault-current. A model of the network is established and also a model for the calculation of the electromagnetic field in the position of the indicator is presented.

Keywords: Compensated Networks, Detection and Location, Earth-Fault, Fault Indicator, Petersen-coil.

I. Introduction

COMPENSATED networks (utilizing resonant grounding) have gained popularity over the last years in distribution networks. This is mainly due to increased focus on reliability of supply. The number of outages is reduced significantly, and thus running expenses for the utility can be brought down. The arc suppression coil was invented by W. Petersen in 1916 [1] as the result of his pioneering work in investigating ground fault phenomena. A well-tuned Petersen-coil compensates for the fault-current and most arcing faults become self-extinguishing. Several methods are utilized in order to detect and locate earth-faults in compensated networks, and are usually classified according to the components of relay input signals:

1. Fundamental frequency
2. Harmonic components
3. Transient components
4. Special methods

The two first groups use steady-state information of the faulted network, and some methods even require pre-fault information. The third group is dealt with in this paper. The last group includes methods that basically use steady-state information, but require control actions on the Petersen coil (current injection or temporary detuning) which is expensive.

E. Bjerkan is with Nortroll AS, Levanger and the Norwegian University of Science and Technology, 7491 Trondheim, Norway (e-mail: ebjerkan@nortroll.no / eilert.bjerkan@elkraft.ntnu.no).

T. Venseth is with Nortroll AS, 7601 Levanger, Norway (e-mail: tvenseth@nortroll.no).

Presented at the International Conference on Power Systems Transients (IPST'05) in Montreal, Canada on June 19-23, 2005
Paper No. IPST05 - 107

Some of the methods have been combined in order to detect and then track down the location of the fault. The most common application is the use of a zero-sequence voltage detector [2] for the connection of a parallel resistor to the Petersen-coil and increase the zero-sequence current in order to apply the watt-metric method [3] for locating the faulty feeder. This is done since the compensated zero-sequence current is too small to be detected reliably compared to system-imbalance.

The discharging/recharging transients during the initiation of the fault can be used to detect the direction to the fault in compensated and isolated networks [4]. The Peterson-coil represents high impedance to the transients. This means the transients are not severely affected and can be applied for fault-locating purposes in compensated and isolated networks.

In rural distribution networks, advanced relaying is normally not prioritized due to rather large investments compared to network income. The sophisticated special methods normally require replacement of both the Peterson coil and its control-system. A system of fault indicators can be an alternative adding to existing relays, it represents minor investments. If the solution is well-planned, it is a cost-effective tool to find faults fast. Engineering an optimal solution with indicators in a network requires detailed knowledge of the network in order to perform network studies and simulations, and to determine the optimized position of every indicator in the network.

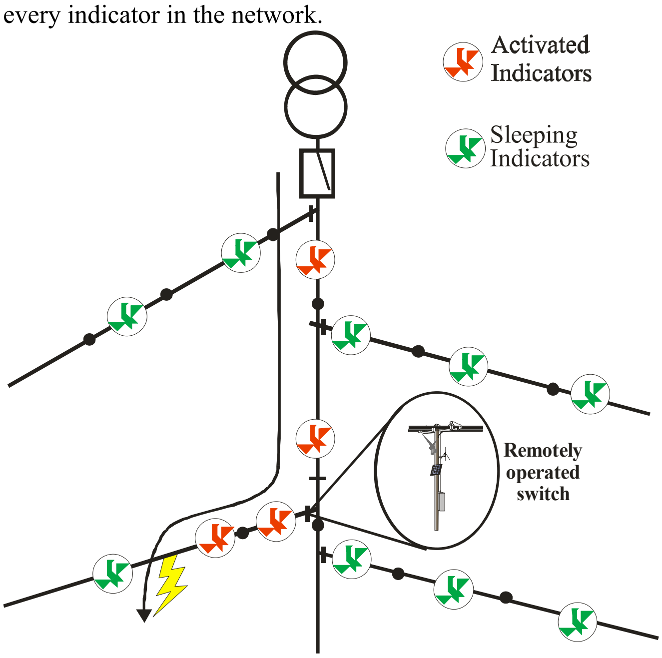

Fig. 1: A typical system of fault indicators in a radial network

The idea is to cover all important sections in a network with fault indicators, in order to determine the faulty section when a fault occurs, ref. Fig. 1. The indicators can either have local indication by means of xenon-flash and high intensity LED's (Light-Emitting Diodes), or by means of remote signalling such as relay contacts, short-distance radio (to a nearby RTU (Remote Terminal Unit)), or a GSM-based system. Signalling from the indicators can be linked up to the SCADA-system of the utility enabling the engineer on duty to make a fast and reliable disconnection of the faulty section by operating the remote-controlled sectionalizing switch closest to the fault. This ensures a fast restoration of the rest of the network if a disconnection has occurred or otherwise will be necessary.

Local automation is another example of a rural application; An indicator is in control of a local motorized recloser. The indicator is programmed to know the sequence of the main circuit-breaker and trips the local recloser during the last (long) disconnection if the fault is detected down-stream of the indicator. The long disconnection indicates a permanent fault.

Fault indicators can be mounted without special equipment and knowledge and without disconnecting the network and thus it lowers the investments (see Fig. 2) compared to other alternatives such as relaying equipment.

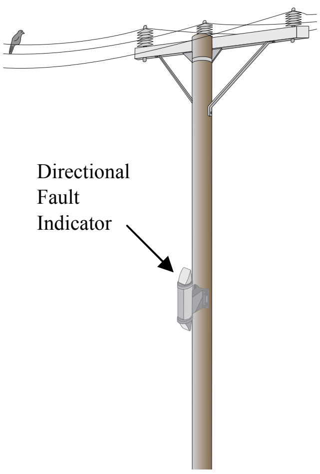

Fig. 2: Pole-mounted directional fault indicator with remote signalling for compensated networks

Travelling waves initiated by earth-faults have long been recognized for fault detection [4], [5] and have been utilized by so-called "Wischer"-relays when other detection-methods have failed in compensated networks. The limitation in this method is that the signals are damped out very fast, and they mainly occur relatively close to the fault-site. Other limitations are challenging sensor-technologies and the high sampling-rate needed in order to measure the signals. Reliability demands multi-terminal measurements synchronized in time, or on a communication channel which makes such solutions suitable only for transmission and not distribution.

The method presented in this paper, make use of the subsequent transient oscillations in order to detect direction to the fault. These transients are slower and the technical requirements of the sensors and equipment are lower, which makes possible the use of self-powered units for distributed measurements such as fault indicators.

The method is not very sensitive to high impedance faults (HIF's), but since the largest share of faults are low impedance faults, a low cost system like this aims at detecting the majority of temporary, restriking- and permanent faults. Detecting HIF in compensated networks is difficult and requires assistance from the special methods mentioned earlier.

II. Theory

The method of detection is based on the making transients due to the establishing of the phase-to-ground fault. A re-distribution of the phase-to-ground voltages is then forced throughout the whole system, with the fault location as the origin of the change.

The making transients can be divided into two components:

- The discharge transient (of the faulty conductor)
- The recharge transient (of the healthy conductors)

The first change concerns the faulty conductor; its charge is drained off, and ground potential is communicated to its entire length. The initial part of this transient is a travelling wave that passes along the faulty conductor (also coupled with the healthy conductors) and discharge it to ground. The termination of the line ends determines the degree of reflection and damping. This transient is also effectively damped out by skin-effect in cables and lines and by the load of the connected distribution-transformers along the line.

The next part of the transient is the recharging of the healthy conductors. This process is less simple since the transport of charge from ground to sound conductors has to be accomplished through the inductance/windings of connected equipment (transformers). This will necessarily be a transient of much lower frequency than the discharge transient. Since the current from this transient must be built up from zero, the charge on the sound conductors are not changed due to the rapid change of the faulty phase. This charge will initiate a damped oscillation into the steady-state fault-situation.

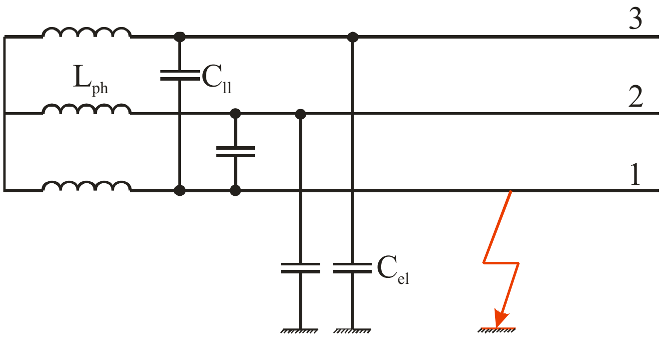

Fig. 3: Equivalent circuit for the recharging transient

As mentioned the recharging currents must flow through the windings of connected transformers (see Fig. 3) and machines. All supply units will act with their short-circuit impedance. Step-down transformers take part in the circuit with their no-load impedance, to which the load forms a parallel path; the inductive component of the latter takes part in the oscillation, the resistive component increases the damping factor. The natural frequency of the recharging transient can be found by considering total inductance and capacitance for the network as in (1). The capacitance considered must be corrected for the imbalance due to the fault.

$$\omega_n = \sqrt{\frac{1}{L_{tot} \cdot C_{tot}}} \tag{1}$$

where L_{tot} is the total inductance as described above. C_{tot} is the total capacitance from the healthy lines to ground. Inter-phase capacitance C_{ll} is neglected, which omit the instantaneous increase in voltage of the healthy lines as discussed by [6]. It is reasonable to assume that L_{tot} and C_{tot} are important in a prospective network simulation model.

The fault indicator measures the electromagnetic field below the line in order to distinguish between faults and other switching operations. It measures the horizontal component of the magnetic field (a substitute for the zero sequence current), and the vertical component of the electrical field (represents the zero sequence voltage).

To establish a link between the network model and the indicators, these fields are estimated by means of superposition: The contribution from each conductor can be summed up to calculate the total electric (see Fig. 4) and magnetic field in the position of the fault indicator.

The magnetic field intensity, **B**, is calculated by means of Ampere's law:

$$\oint \mathbf{B} \cdot d\mathbf{s} = B \cdot 2\pi r = \mu_0 I \rightarrow B = \frac{\mu_0 I}{2\pi r} \tag{2}$$

Since the horizontal component is required, (3) is applied to describe the total field intensity in the point (x, y) of the indicator for a set of n conductors in the positions (x_i, y_i):

$$B_x = \sum_{i=1}^{n} \left[-\frac{\mu_0 I_i}{2\pi} \cdot \frac{(y - y_i)}{(x - x_i)^2 + (y - y_i)^2} \right] \tag{3}$$

The current I_i of each conductor flows in the z-direction (into the paper plane). The induced currents in the ground are not accounted for since the lossy ground properties determine the depth of the mirror-currents, and complicate calculation.

The electrical field-strength, **E**, in (x, y) is derived from Gauss' law and the vertical component is found by:

$$E_y = \sum_{i=1}^{m} \left[\frac{\varepsilon_0 \cdot q_i}{2\pi} \cdot \frac{y - y_i}{(x - x_i)^2 + (y - y_i)^2} \right] \tag{4}$$

Since the conductor voltage is known, the individual linear charge densities (including the mirror-charges as shown in Fig. 4) can be derived by determining the potential-coefficients as shown in Appendix A. Ground conductors and shielding lines can also be included by applying ground potential. The pole will also influence the measured electrical field but requires investigations in terms of 3D FEM-calculations.

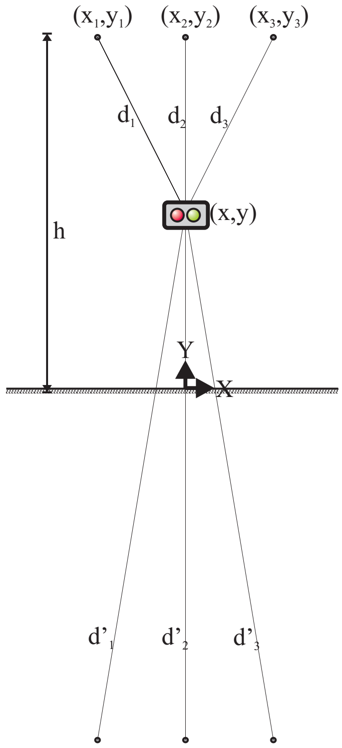

Fig. 4: Electrostatic contribution from conductors and their mirror-charges

The operation of the fault indicator is based on a comparison of the polarity between the measured voltage- (vertical component of electrical field: E_y) and current-transient (horizontal component of flux density: B_x) as shown below. If the two transients are in phase, the fault is considered to be a forward fault (downstream if the indicator is facing the feeder), and if the two transients are in opposite phase, the fault is considered a backward fault (upstream), ref. Fig. 5:

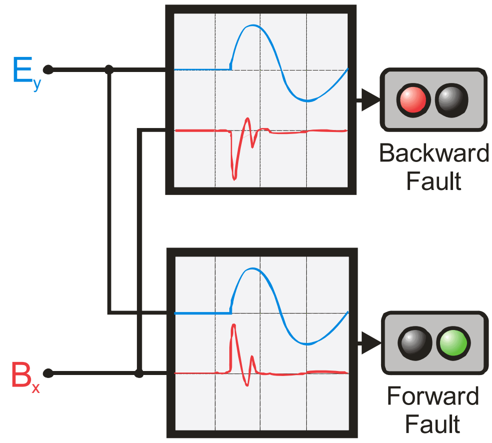

Fig. 5: Functional description of the directional fault detection routine

The polarity of the measured magnetic field density, B_x, is dependent on the orientation of the pickup-coil used as sensor.

III. Measurements

The distribution network selected for the field test is a typical rural distribution network in Norway (see Fig. 6).

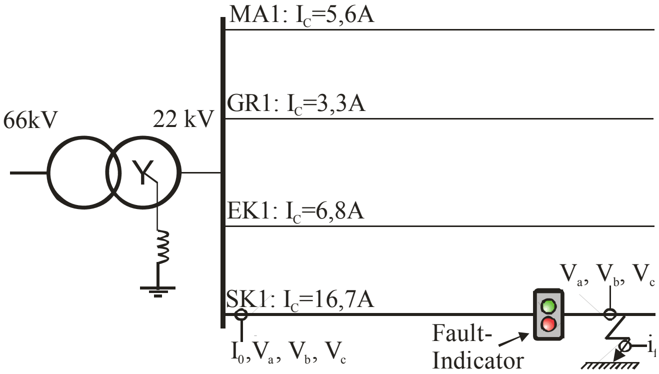

Fig. 6: Diagram of the distribution network for the field test.

The network holds mostly overhead lines, but a small town centre is supplied by a cable network. The location of the fault is situated at the transition from OH-line to the cable-network of this town-centre at the end of the feeder named *SK1*. The lengths and types are elucidated in TABLE I.

TABLE I
TYPES AND LENGTHS OF THE DIFFERENT FEEDERS IN THE TESTED NETWORK

Name of Feeder	Overhead Lines	Cables
MA1	48,6 km	1521 m
GR1	26,9 km	887 m
EK1	44,8 km	1300 m
SK1	11,9 km	7316 m
Total:	**132.2 km**	**11024 m**

The total stationary non-compensated earth-fault-current is 32,4 A. This network is normally 20% overcompensated so a compensated fault-current of 6,5 A is expected. Shunt losses and series-resistance of the Peterson-coil raises this number to a certain extent. In addition networks are never fully transposed.

For measuring the phase voltages and zero-sequence currents in the substation and at the fault site, transient recorders and wide band current transformers were used (Pearson current monitors [7]), in addition to capacitive voltage dividers for accurate voltage measurements.

Measurements are done with and without compensation, but the shape of the transients is generally the same so this paper only shows the measurements from the compensated network. The big difference is the arc-quenching and re-ignitions.

The earth-fault is applied using custom-built equipment. The apparatus is mounted on a pole using a rope and pulley as shown in Fig. 7. The alternative is a circuit-breaker and a sphere gap, but the mobility during field tests is limited.

The fault resistor is made up of a cylindrical water-tank (PVC-tube; can be seen in the lower part of Fig. 8 at the base of the pole) where the resistance is controlled by the addition of sodium chloride into the water. The advantage of using ionized water is the large heat capacity resulting in a small and mobile fault-resistor with high power ratings.

Fig. 7: Apparatus for applying the earth-fault

This enables the operator to apply the fault from a safe distance by pulling the rope as shown in Fig. 8. In this way the fault is made arcing and a fault close to zero-crossing of the voltage is avoided.

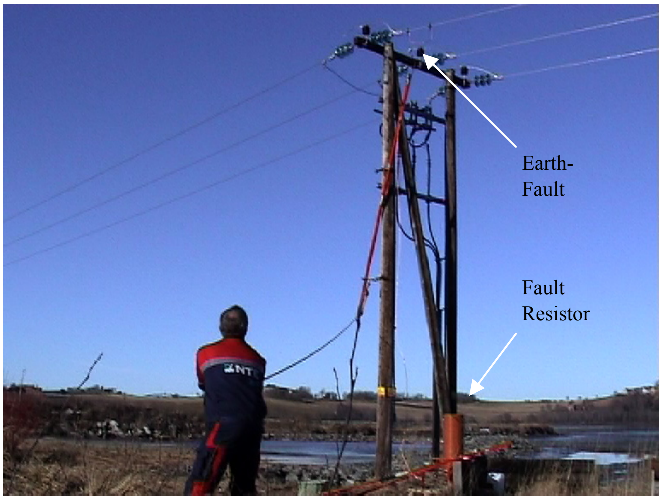

Fig. 8: Safe operation of the grounding apparatus

A comparison between measurements and the developed network model is shown in the following. First the measured phase to ground voltages at the fault-site are shown in Fig. 9.

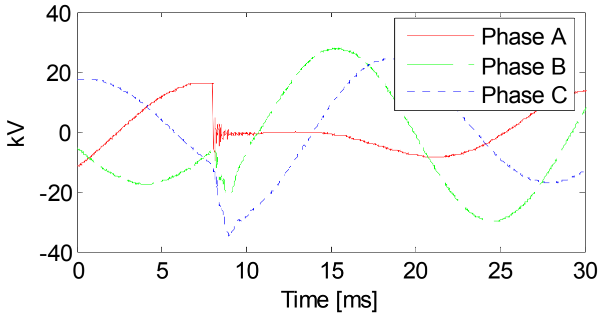

Fig. 9: Measured phase to ground voltages at fault-site

The measured phase-to-ground voltages at the fault site, are summed to obtain the zero-sequence voltage in Fig. 10:

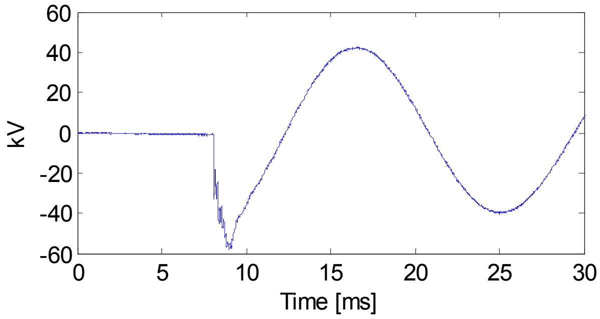

Fig. 10: Zero-sequence voltage calculated from the sum of phase voltages

The next measurement of interest is the fault-current as shown in Fig. 11:

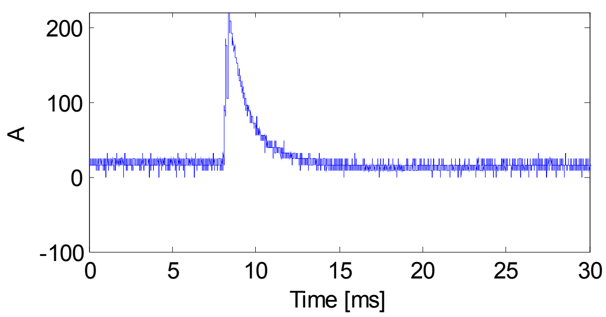

Fig. 11: Measured fault-current

Unfortunately the measurement of the current suffers from low resolution, but is still comparable with simulations.

IV. Network Model

A simple model is developed in ATP [8] for the network being tested. The overhead lines are modelled using the Bergeron-model, while cable networks are implemented by using a transposed, distributed parameter line (Clarke) since most of the cable segments are short. The damping of the Bergeron-model in this application might be too low, but since this is an initial model made for verifying a principle rather than amplitudes and frequency, it is chosen as a start.

The main transformer is included by means of a BCTRAN-model based on test-record data. The transformer is a 25 MVA 63/22 kV YNyn0. All measurements and simulations shown are done using a fault-resistance of 20 Ω. Fig. 12 shows the simulated phase to ground voltages.

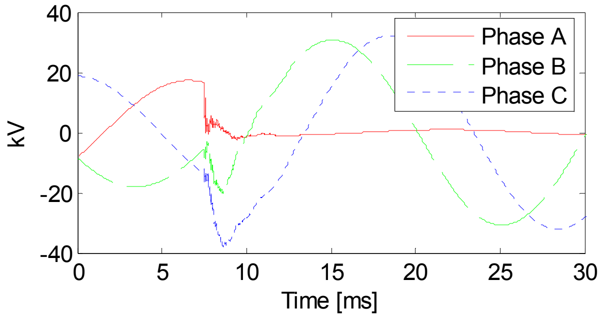

Fig. 12: Simulated phase to ground voltages at fault-site

Coherence between Fig. 9 to Fig. 12 is close. The simulated zero-sequence voltage is shown in Fig. 13.

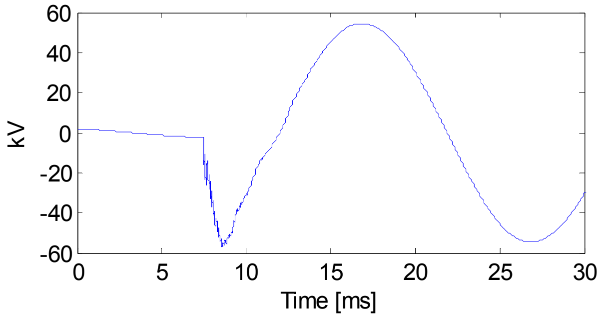

Fig. 13: Simulated zero-sequence voltage

The simulated fault-current (Fig. 14) does not coincide as well to the measurement (Fig. 11) as the voltages.

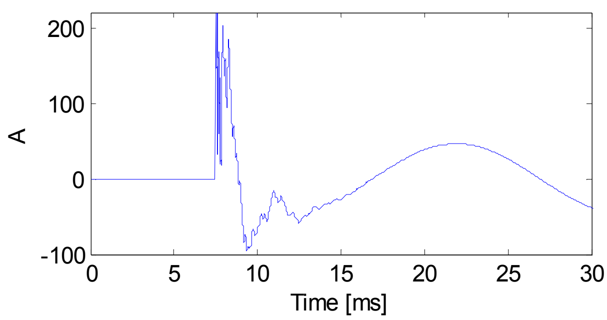

Fig. 14: Simulated fault-current

V. Indicator Model

A model for the indicator using (3) and (4) was developed using MODELS [9]. The result of applying this model into the network model for a forward fault is shown in Fig. 15:

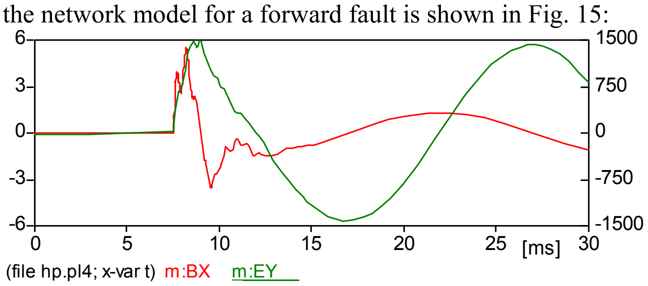

Fig. 15: Model results for Bx in [uT] and Ey in [V/m]

A backward fault will be similar but have the opposite polarity for B_x and is therefore not shown.

VI. Discussion

Some fundamental assumptions are made in this paper, which more or less influence on the results:

- A very simple approach is chosen for the overhead line. Frequency-dependent losses will not be included properly (especially for zero-zequence mode). A simple test with a Jmarti-model improved the damping of the fault-current compared to measurements.
- Cable-types are not known and some of them are modeled with their respective surge-impedance. The losses are implemented on a lumped basis. The rest of the contributions from the cables are represented as lumped capacitances throughout the network.
- Resistive component for Petersen-coil is neglected. The arc-quenching is not modeled, and this is a possible explanation for difference between the measured and simulated fault current, see Fig. 11 & Fig. 14.
- Distribution transformers are not loaded and only a few are modeled. This seems important for the appearance of the recharging-transient in the fault-current.

VII. Conclusions

The presented paper shows a comparison between a network model and measurements during a live earth-fault test. Coherence is adequate to test and verify the theory of using the recharging transients to detect and locate earth-faults. Simulations of the studied network have shown that faults with resistance up to 1kΩ can be detected by this principle in this specific network. The Petersen-coil does not change zero-sequence signals significantly. Fault indicators constitute a cost-effective fault-locating solution with capabilities of local automation and remote signalling.

The developed model for the electromagnetic field parameters in the mounting-position of the indicator helps evaluation of the measured signals compared to zero-sequence signals. If the distance from the line is large compared to the horizontal distance between the outer conductors, the measured signals can be equalized to the zero-sequence current and voltage, neglecting image currents and 3D-effects.

VIII. Appendix

A. Determination of the potential coefficients

The matrix of potential coefficients are determined from the contribution to the potential in *(x,y)* of the charge densities q_i for all the conductors referred to Fig. 4, including mutual effects. When $i \neq j$ the coefficients are given as:

$$\beta_{ij} = \frac{\varepsilon_0}{2\pi} \cdot \ln\left\{ \sqrt{\frac{(x_i - x_j)^2 + (y_i + y_j)^2}{(x_i - x_j)^2 + (y_i - y_j)^2}} \right\} \qquad \text{(A.1)}$$

For $i = j$ the coefficients are:

$$\beta_{ii} = \frac{\varepsilon_0}{2\pi} \cdot \ln\left\{ \frac{2h_i}{r_i} \right\} \qquad \text{(A.2)}$$

where h_i is the height above ground for conductor i, and r_i is the radius of the same conductor. The line-charges can then be derived using these coefficients and the phase-voltages:

$$\mathbf{q} = \boldsymbol{\beta}^{-1} \cdot \mathbf{V} \qquad \text{(A.3)}$$

IX. Acknowledgment

The authors gratefully acknowledge the help and support from the local utility NTE (Nord-Trøndelag Elektrisitetsverk) during the field tests in their distribution networks in Skogn and Levanger. Gratitude is also expressed to Sintef Energy Research for conducting the measurements during the field tests, and participating in the development of the fault-resistor.

X. References

[1] W. Petersen, "Neutralizing of Ground Fault Currents and Suppression of Ground Fault Arcs through the Ground Fault Reactor", *E.T.Z.*, 40 (1916) 5, 17.

[2] E. T. B. Gross, "Sensitive Fault Protection for Transmission Lines and Distribution Feeders," *AIEE Transactions*, Vol. 60, Nov. 1941, pp. 968–972.

[3] L. F. Hunt and J. H. Vivian, "Sensitive Ground Protection for Radial Distribution Feeders", *AIEE Transactions*, Vol. 59, February 1940, pp. 84–90.

[4] S. Margoulies, P. Fourmarier, "The Location of Faults on Overhead Lines by Means of Impulse Waves", *CIGRE*, 12th Session (1948), Report 307

[5] L. J. Lewis, "Travelling wave relations applicable to power-system fault locators", *AIEE Trans*. Vol. 70, 1951, pp. 1671-1680

[6] R. Willheim, M. Waters, *Neutral grounding in high-voltage transmission,* New York: Elsevier, 1956, 670 pages

[7] Pearson Electronics Inc., "Standard Current Monitors," Online: http://www.pearsonelectronics.com

[8] *Alternative Transients Program (ATP) - Rule Book*, Canadian/American EMTP User Group, 1987-1998.

[9] L. Dubè, I. Bonfanti, "MODELS: A new simulation tool in the EMTP". *European Trans. on Electric Power*, vol. 2, no. 1, pp.45-50, Jan./Feb. 1992.

XI. Biographies

Eilert Bjerkan was born at Frosta, Norway in 1973. He received his B.S. degree in electrical engineering from the Nord-Trøndelag University College and his M.S. degree from the Norwegian University of Science and Technology, in 1995 and 1998 respectively. He is currently working towards his Ph.D. degree at the Norwegian University of Science and Technology, dept. for Electrical Power Engineering.

He has been working as R&D-engineer at Nortroll AS, Levanger before starting his Ph.D.-work. His main interests of research include power transformer modeling, condition assessment, finite element calculations and power network transients.

Terje Venseth was born in Levanger, Norway in 1963. He received his B.S. Degree in electrical engineering from the Trondheim Technical College in 1985, and the M.S. degree from the Norwegian University of Science and Technology in 1995.

He has been involved in R&D in Nortroll AS, Levanger since 1986 and is currently R&D Manager in the same company.